

Development of an algorithm using zernike polynomials and fourier transform for measuring refractive errors in the human eyes

Marie Cattleah D. Atas, Larish Mariam T. Landicho, Abigail D. Lobo, Carla Joy L. Orubia, Adolph Christian O. Silverio, and John Carlo V. Puno*

Abstract— This study aims to develop an algorithm using Zernike polynomials and Fourier transform to provide a reliable measurement of refractive errors that will aid ophthalmologists and optometrists. A Shack-Hartmann wavefront sensor captures the wavefront of the eyes and provides the raw image that will be processed. The Fast Fourier Transform (FFT) of the image is computed and the magnitude and phase spectrum from two peaks surrounding the DC frequency are generated. These values are correlated and computations using formula for Zernike polynomials are performed. The outputs are spherical (SPH), cylindrical (CYL), and axial (AX) values which represent the refractive errors of the eyes. The results are displayed in the device and uploaded to a database which can be viewed at the website online. The device was able to provide a reliable measurement which can aid in conducting eye checkups. With this, refractive errors may be detected and corrected at an early stage to prevent severe vision impairments.

Keywords— (*Refractive Error, Adaptive Optics, Wavefront Technology, Shack-Hartmann Wavefront sensor, Zernike Polynomials, Fast Fourier Transform, Confusion Matrix*)

I. INTRODUCTION

The human eye is an optical system that converts the light rays into messages that the brain interprets into images. Imperfections in the human eye cause the light rays to deviate and impair the quality of vision. This result to optical or wavefront aberrations which can be classified as lower-order or higher-order aberrations. The lower-order aberrations (LOA) describe the refractive errors of the human eyes. These LOA can be classified as myopia or commonly known as myopia, hyperopia or farsightedness, and astigmatism. [1][2]

Several innovative approaches have been developed in the field of ophthalmology in order to measure the refractive error of the human eyes [3][4]. One of the early methods incorporate the use of Snellen charts and phoropters. The Snellen charts are used to measure the visual acuity by having the patient identify letters from the chart within a certain distance. The eye specialist fine-tunes the prescription using phoropter and asks the patient which set of lenses gives the sharpest vision. [5][6] These methods, however, are subjective since it depends solely on the feedback of the patient [7].

Over the last two decades, techniques of adaptive optics made way to the expansion of the wavefront-related technologies [3][4]. Through wavefront technology, the measurement of the refractive errors became objective, rather than subjective [7]. The most popular method being used currently is the Shack-Hartmann method [3]. In this study, an algorithm for identifying the degree of lower-order aberrations in the eyes using the raw image from a Shack-Hartmann wavefront sensor is developed through the use of Zernike polynomials and Fast Fourier Transform.

II. THEORETICAL BACKGROUND

Refractive errors, when left uncorrected, may lead to severe vision impairments and in worst cases, may lead to blindness. Limited availability and the affordability of the eye checkups lead to a lot of people who suffers to poor eyesight. The World Health Organization (WHO) said that providing effective and accessible eye care services is the key to solve the problem with uncorrected refractive errors. [8][9] [10]

The imperfections in the human eye can now be measured more efficiently through wavefront aberrometry. Wavefront describes these imperfections objectively by how the light traveled through the eyes. Since then, expressing these aberrations using mathematical equations has become necessary. Various reconstruction techniques were developed in order to describe the wavefront of the eyes and quantify the refractive errors present. These include the Zernike polynomials and Fourier transform. Before performing mathematical techniques, wave aberrations in the eyes

* John Carlo V. Puno, Electronics Engineering Department
Technological University of the Philippines, Manila,
Philippines (email: jcp040195@gmail.com)

are sensed using an apparatus such as the Shack-Hartmann sensor. [3][11]

A. Shack-Hartmann Wavefront Sensor

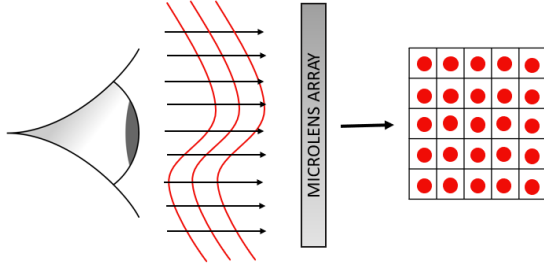


Fig. 1. Principle of the Shack-Hartmann Wavefront Sensor

The Shack-Hartmann wavefront sensor was developed in the late 1960's by the University of Arizona. It was originally purposed for large telescopes to resolve the problem with atmospheric turbulence. The sensor was first used for ophthalmic application in the mid-1980's. This led to the advancements in the treatment of the refractive errors and other applications that helped in the field of ophthalmology. [12][13]

The Shack-Hartmann wavefront sensor measures the aberrations through the outgoing light being reflected by the retina. It is mainly composed of the microlens array and the charge-coupled device (CCD). The microlens array focuses the light as it is subdivided into small beams to the CCD array. [4][14] The CCD camera then captures the wavefront of light, providing the raw data containing red dots. Figure 1 shows the principle of the Shack-Hartmann wavefront sensor. The output, which serves as the raw data will be analyzed mathematically to quantify the refractive errors present in the eyes.

B. Zernike Polynomials

Zernike polynomials are often defined as a complete set of orthogonal polynomials inside a unit circle domain. The shape of the wavefront can be analyzed by expanding it into sets of Zernike polynomials. The Zernike expansion is a well-established method for reconstructing the wavefront aberrations in the field of optics. [15][16]

TABLE I
ZERNIKE POLYNOMIALS IN POLAR COORDINATES

#	n	m	Polynomial
0	0	0	1
1	1	1	$\rho \cos(\theta)$
2	1	-1	$\rho \sin(\theta)$
3	2	0	$-1+2\rho^2$
4	2	2	$\cos(2\theta)$
5	2	-2	$\sin(2\theta)$

The degrees of the polynomials may be classified as a lower-order aberration or a higher-order aberration. The lower-order aberrations comprise the spherocylindrical

or refractive errors present in the eyes [17]. The Zernike polynomials, as used in this study and shown in Table 1, are usually expressed in polar coordinates [18].

C. Fast Fourier Transform

When defocus occurs in the eyes, measuring the refractive error by calculating the displacements of the spots in the Shack-Hartmann grid becomes unclear. Using the Fourier transform models the image as a two-dimensional array of delta functions in the frequency domain. Using Fourier analysis provides a wide-ranging evaluation for every single spot in the Fourier space contains all information about the pupil. [16][19]

Using two peaks from the Fourier transformed image, it is possible to compute for the refractive errors. Any two peaks from the central of DC frequency may be used. Noise tends to get pushed to the edge of the Fourier image since it has higher frequencies, therefore making the surrounding peaks free from being corrupted. [19] Correlating the two values obtained from the Fourier transformed image will provide the values of spherical, cylindrical, and axis.

III. METHODOLOGY

This section explains the procedures used to develop the algorithm for measuring refractive errors in the human eyes.

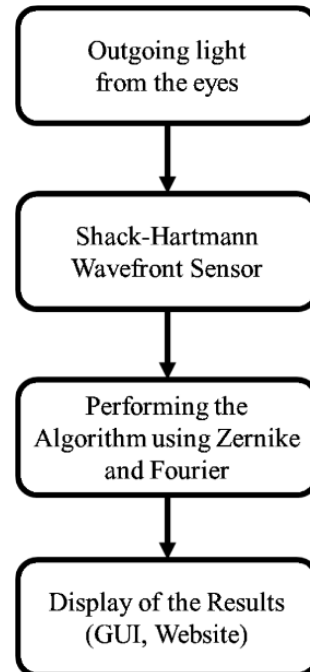


Fig. 2. System Block Diagram

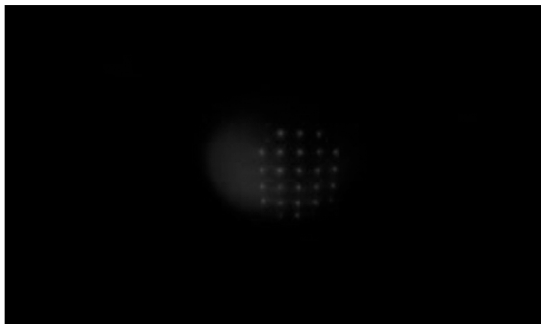


Fig. 3. Raw image from the Wavefront Sensor

Figure 2 shows the general block diagram of the whole process. The input is the outgoing light from the human eye. The Shack-Hartmann wavefront sensor captures the wave aberrations from the eyes. The output, as shown in Figure 3, will serve as the raw image for performing the algorithm. The raw image shows the light pattern that will be generated as the light from the device strikes to the eyes of the subject.

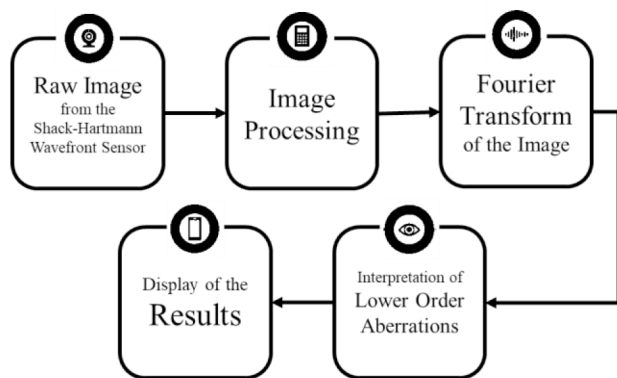
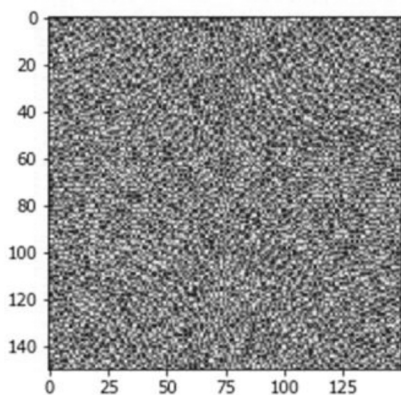
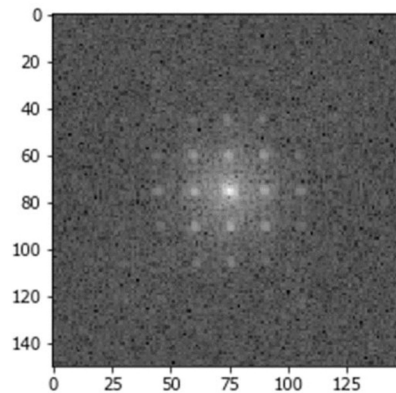


Fig. 4. Block diagram of the Algorithm

Figure 4 shows the process of performing the algorithm on the raw image obtained from the Shack-Hartmann wavefront sensor. Before executing the Fourier transform, the image is processed to reduce the noise. Gaussian filtering smoothens the image and is highly effective in eliminating Gaussian noise. [20] The median filter is also applied to further improve the image. After these processes, the filtered image will be reconstructed using the fast Fourier transform.



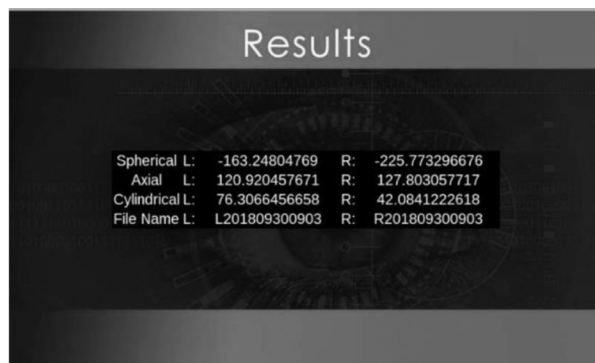
(a)



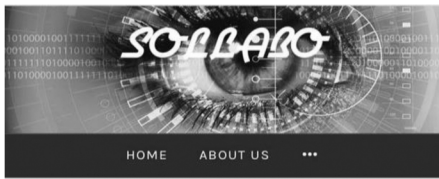
(b)

Fig. 5. (a) Phase spectrum (b) Magnitude spectrum

The phase (Fig 5.a) and magnitude (Fig 5.b) spectrum are generated from the Fourier transform image. From the central peak, two peaks were chosen, and the values of those two peaks were obtained. The correlations of these two values will be used in some mathematical computations using Zernike polynomials. From these, the values of the refractive errors are obtained. These are the spherical (SPH), cylindrical (CYL) and axial (AX) values, respectively.



(a)



Results

SOLLABO_Results : Data

File Name	SPH	CYL	
L201901161455	-19.18122087	-0.3221920024	12
R201901161455	-213.5620615	27.42660163	13
L201901161456	-8.136960861	3.100787304	45
R201901161457	-7.63295223	2.667385992	45
L201901161457	-194.4686255	24.77584927	13
R201901161458	-72.47130671	23.11531159	12
L201901161458	-819.7951087	452.9883875	12
R201901161459	-31.36021743	0.9375925046	1
L201901161459	-108.8729145	12.14411089	13
R201901161500	-442.652064	102.8597954	12
L201901161501	-76.80732931	7.405518013	1
R201901161501	-42.02232465	4.667509213	12
L201901161503	-118.5683591	13.7537795	13
R201901161504	-60.51372408	6.906974192	12
L201901161505	-510.9748265	71.40127347	13
R201901161505	-18.22589017	-1.051017547	13

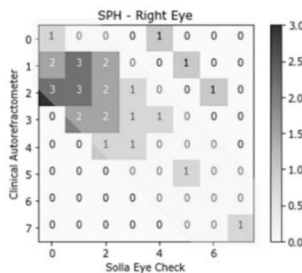
(b)

Fig. 6. Sample result from the (a) GUI (b) website

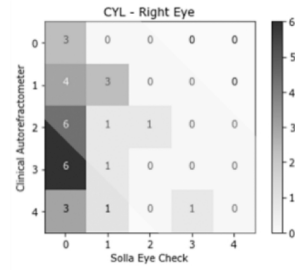
After the conducting an eye checkup, results can be seen through the graphical user interface (GUI) of the Shack-Hartmann wavefront sensor as shown in Figure 6.a. The parameters, SPH, CYL, and AX for both the left and right eyes are displayed as well as the filename that is assigned for every checkup of the eye. The filename serves as the reference for the users when they access the checkup results in the website as seen in Figure 6.b. The website is accessible as soon as the user has access to the internet. The results are uploaded and updated in real-time.

IV. RESULTS

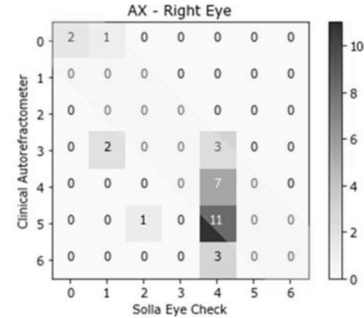
The results and evaluation of the algorithm for measuring refractive errors using Zernike polynomials and Fourier transform are explained in this section.



(a)



(b)



(c)

Fig. 7. Confusion matrix representation of values for (a) spherical (b) cylindrical (c) axial

Confusion matrix allows data to be analyzed by comparing it to the true values. [21] To assess the reliability of the algorithm for the Shack-Hartmann wavefront sensor, refractive errors of 30 people were gathered. Figure 10 shows the result of the comparison of the clinical autorefractometer and SOLLA Eye Check using confusion matrix. Since results from autorefractometers are affected by various factors and varies up to $\pm 0.50D$ [22][23], the true positives included the yellow-shaded area of the confusion matrix. The clinical results serve as the true or actual value while the results from the algorithm for the wavefront sensor serve as the predicted values.

TABLE II
SPHERICAL VALUES

Measure	Calculated Values
Accuracy	0.9
Misclassification Rate	0.1
Miss Rate (False Negative Rate)	0
Fall-out (False Positive Rate)	0.4286

TABLE III
CYLINDRICAL VALUES

Measure	Calculated Values
Accuracy	0.6667
Misclassification Rate	0.3333
Miss Rate (False Negative Rate)	0.3448
Fall-out (False Positive Rate)	0

TABLE IV
AXIAL VALUES

Measure	Calculated Values
Accuracy	0.8
Misclassification Rate	0.2
Miss Rate (False Negative Rate)	0.6667
Fall-out (False Positive Rate)	0

There are many measures that can be used to interpret the confusion matrix. Among these are the accuracy, misclassification or error rate, miss rate, and fall-out rate [24]. These measures are applicable for this study. The accuracy rate shows what percentage of the data gathered matched the results of the clinical autorefractometer within the range of $\pm 0.50D$, while the misclassification or error rate shows the percentage that weren't in the acceptable range. The miss rate, also known as the false negative rate, shows the times that the autorefractometer has a high result but the algorithm yielded a lower result. On the other hand, fall-out rate, also known as the false positive or false-alarm rate, shows the times that the predicted values were higher than the actual values. Tables 2-4 shows the calculated values using the different measures mentioned.

Based on the analysis of the confusion matrix, the accuracy of the algorithm for the wavefront sensor is about 0.7889 or 78.89% and the misclassification rate is about 0.2111 or 21.11%. The average miss rate is 0.3371 or 33.71% and the average fall-out rate is 0.1429 or 14.29%. Hence, the prototype may be used as basis for eye checkups.

V. CONCLUSION

The algorithm developed using Zernike polynomials and Fourier transform for the Shack-Hartmann wavefront sensor was able to give reliable results for eye checkups. The Fourier transform can be used to analyze the wavefront errors of the eyes instead of iterating and computing values of spot displacements in the CCD space. The correlation of the two peak values from the Fourier space can be used for Zernike computations to yield the refractive errors of the eyes. The results of statistical analysis show that the algorithm successfully extracted the values of the spherical, cylindrical, and axial errors using the device through the image generated from the sensor.

With the use of the prototype, the refractive errors may be detected at an early stage. The immediate correction of refractive errors will avoid more problems that may occur most specially to lower aged users. This prototype will provide low-cost but efficient and highly-accessible eye care service.

VI. FUTURE WORKS

The proponents suggest in using a Shack-Hartmann wavefront sensor that give a high-definition image as an output. It is also recommended to use a better microcontroller for high-speed processing. Furthermore, the researchers suggest that the factors affecting the eye checkups be considered. The patient should not be dizzy or tired and other light sources aside from the light reflected by the retina of the patient's eyes should be prevented from being captured by the Shack-Hartmann wavefront sensor.

ACKNOWLEDGMENT

The researchers would like to extend their gratitude to an Ophthalmologist from the UST Hospital, Dr. Alex Gungab in sharing his knowledge and expertise in the field. Also to the Local Government Unit of Barangay Paso de Blas in Valenzuela City for providing comments and letting the researchers to deploy the project.

REFERENCES

- [1] M. Resan, M. Vukosavljevi and M. Milivojevi, "Wavefront Aberrations", *Advances in Ophthalmology*, 2012. Available: 10.5772/24441
- [2] "Facts About Refractive Errors | National Eye Institute", *nei.nih.gov*, 2010. [Online]. Available: <https://nei.nih.gov/health/errors/errors>.
- [3] M. Parthasarathy and V. Lakshminarayanan, "A Brief History of Aberrometry Applications in Ophthalmology and Vision Science", *Springer Proceedings in Physics*, pp. 31-39, 2017. Available: 10.1007/978-981-10-3908-9_4
- [4] M. Lombardo and G. Lombardo, "New methods and techniques for sensing the wave aberrations of human eyes", *Clinical and Experimental Optometry*, vol. 92, no. 3, pp. 176-186, 2009. Available: 10.1111/j.1444-0938.2009.00356.x
- [5] A. Wallerstein, "Aberrometry and Wavefront Imaging: Historical Perspective, Wavefront Error, Optical Aberrations of the Eye", *emedicine.medscape.com*, 2016. [Online]. Available: <https://emedicine.medscape.com/article/1228601-overview>.
- [6] "Eye exam - Mayo Clinic", *mayoclinic.org*, 2018. [Online]. Available: <https://www.mayoclinic.org/tests-procedures/eye-exam/about/pac-20384655>.
- [7] Smart Visions Lab. "Wavefront technology is the wave of the future" Available [Online] <https://www.smartvisionlabs.com/blog/wavefront-technology-is-the-wave-of-the-future/>.
- [8] "Uncorrected Refractive Error | Lions Clubs International", *lionsclubs.org*, 2019. [Online]. Available: <https://lionsclubs.org/en/resources-for-members/resource-center/uncorrected-refractive-error>.
- [9] *Universal eye health*. Geneva: World Health Organization, 2013.
- [10] "Vision impairment and blindness", *who.int*, 2018. [Online]. Available: <https://www.who.int/news-room/fact-sheets/detail/blindness-and-visual-impairment>.
- [11] G. Yoon, S. Pantanelli and S. Macrae, "Comparison of Zernike and Fourier wavefront reconstruction algorithms in representing the corneal aberration of normal and abnormal eyes", *Journal of Refractive Surgery*, Thorofare, N.J. : 1995, 24, pp. 582-90.
- [12] Schwiegerling, "History of the Shack Hartmann wavefront sensor and its impact in ophthalmic optics", *Fifty Years of Optical Sciences at The University of Arizona*, 2014. Available: 10.1117/12.2064536.
- [13] J. Schwiegerling and D. Neal, *Historical Development of the Shack-Hartmann Wavefront Sensor*. 2005.

- [14] F. Cade, A. Cruzat, E. Paschalis, L. Espírito Santo and R. Pineda, "Analysis of Four Aberrometers for Evaluating Lower and Higher Order Aberrations", *PLoS ONE*, vol. 8, no. 1, p. e54990, 2013. Available: 10.1371/journal.pone.0054990.
- [15] L. Carvalho, "Accuracy of Zernike Polynomials in Characterizing Optical Aberrations and the Corneal Surface of the Eye", *Investigative Ophthalmology & Visual Science*, vol. 46, no. 6, p. 1915, 2005. Available: 10.1167/iovs.04-1222
- [16] M. Jesson, A. Pachiyappan and A. Ganesan, *Analysis of Refractive errors in the human eye using Shack Hartmann Aberrometry*. 2019.
- [17] N. Maeda, "Clinical applications of wavefront aberrometry - a review", *Clinical & Experimental Ophthalmology*, vol. 37, no. 1, pp. 118-129, 2009. Available: 10.1111/j.1442-9071.2009.02005.x.
- [18] P. Maeda, "Zernike polynomials and their use in describing the wavefront aberrations of the human eye", Stanford University, 2003.
- [19] J. Beverage, "Measuring refractive error in the human eye using a Shack-Hartmann-based autorefractor", Ph.D., Doctoral, University of Arizona, 2003.
- [20] "Smoothing Images — OpenCV 2.4.13.7 documentation", *Docs.opencv.org*, 2019. [Online]. Available: https://docs.opencv.org/2.4/doc/tutorials/imgproc/median_blur_bilateral_filter/median_blur_bilateral_filter.html.
- [21] "Basic evaluation measures from the confusion matrix", *Classifier evaluation with imbalanced datasets*, 2015. [Online]. Available: <https://classeeval.wordpress.com/introduction/basic-evaluation-measures/>.
- [22] N. Strang, L. Gray, B. Winn and J. Pugh, "Clinical evaluation of patient tolerance to autorefractor prescriptions", *Clinical and Experimental Optometry*, vol. 81, no. 3, pp. 112-118. Available: 10.1111/j.1444-0938.1998.tb06729.x.
- [23] "You Can Visit Two Eye Doctors and Get TWO Different Prescriptions, Here's Why", EyeQue, 2018. [Online]. Available: <https://www.eyequ.com/knowledge-center/you-can-visit-two-eye-doctors-and-get-two-different-prescriptions-heres-why/>.
- [24] M. Mishra, "Simplifying The Confusion Matrix – Data Driven Investor – Medium", *Medium*, 2018. [Online]. Available: <https://medium.com/datadriveninvestor/simplifying-the-confusion-matrix-aal1fa0b0fc35>.